The Journal of Chemical Physics ARTICLE scitation.org/journal/jcp

On delicate balance between formation and decay of tetracyanoethylene molecular anion triggered by resonance electron attachment

Cite as: J. Chem. Phys. 158, 164309 (2023); doi: 10.1063/5.0149262
Submitted: 5 March 2023 • Accepted: 12 April 2023 •
Published Online: 28 April 2023

Stanislav A. Pshenichnyuk,[1,a)] Nail L. Asfandiarov,[1] Rustam G. Rakhmeyev,[1] Aleksey M. Safronov,[1] and Alexei S. Komolov[2]

AFFILIATIONS

[1] Institute of Molecule and Crystal Physics, Ufa Federal Research Centre, Russian Academy of Sciences, Prospekt Oktyabrya 151, 450075 Ufa, Russia

[2] St. Petersburg State University, Universitetskaya nab. 7/9, 199034 St. Petersburg, Russia

[a)] **Author to whom correspondence should be addressed:** sapsh@anrb.ru

ABSTRACT

Low-energy (0–15 eV) resonance electron interaction with isolated tetracyanoethylene (TCNE) molecules is studied *in vacuo* by means of dissociative electron attachment (DEA) spectroscopy. Despite this molecule being relatively small, the long-lived molecular anions $TCNE^-$ are formed not only at thermal electron energy via a vibrational Feshbach resonance mechanism but also via shape resonances with the occupation of the π_4^* and π_5^* molecular orbitals by an incident electron. Dissociative decays of $TCNE^-$ are mostly observed at incident electron energy above the π_7^* temporary anion state predicted to lie at 1.69 eV by means of B3LYP/6-31G(d) calculations combined with the empirical scaling procedure. Electron attachment to the π_6^* orbital (predicted at 0.85 eV) leads to the generation of long-lived $TCNE^-$ species, which can decay via two competing processes: extra electron detachment, which appears in hundreds of microseconds, or elimination of two cyano groups to form the $[TCNE - 2(CN)]^-$ negative fragment on a tens of microsecond timescale. The latter is accompanied by the generation of a highly toxic cyanogen molecule as a neutral counterpart. Since the electron transfer to the acceptor molecule TCNE plays a key role in the formation of single-molecule magnets, the present data are of importance to understand the long-term behavior and likely harmful effects produced by cyanide-based prospective materials.

I. INTRODUCTION

Elementary electron-induced processes, in particular resonance dissociative electron attachment (DEA),[1–3] occurring in microscopic systems, are of great importance to understand more complex phenomena observed in a variety of natural[4–6] and artificial[7–9] molecular assemblies containing structural elements characterized by high electron affinity.[10,11] Disclosing the fundamental mechanisms of low-energy (0–15 eV) electron-driven reactions in polyatomic molecules requires a deep understanding of the dynamics of simple model structures bearing an excess electron.[12,13] Cyano-containing compounds are usually characterized by high electron-withdrawing ability[10,11] and attract much attention due to their prospective application in nanoscale organic electronics.[14–16] The biological impact of cyanides is due to their strong toxic activity against living organisms[17,18] as well as their likely pharmacological properties,[19] the latter of which is linked with the mystery of cyanide production by cyanogenic plants.[20]

Tetracyanoethylene (TCNE; see structure reported in Fig. 1), a molecule containing as many as four cyano groups, has been considered a promising structural element in the molecular magnet technology,[21,22] where controlled electron transport through magnetically ordered molecules is required. In fact, electron transfer from the metal to the acceptor molecule has been found[21] to be responsible for the formation of the genuine metal-cyanide molecular magnet and, moreover, plays an important role in magnetic ordering.[22] Therefore, the energy alignment of vacant molecular orbitals and the dynamics of the TCNE negative ion are of much interest to understand the long-term behavior of TCNE-based magnetically ordered nanoscale structures.

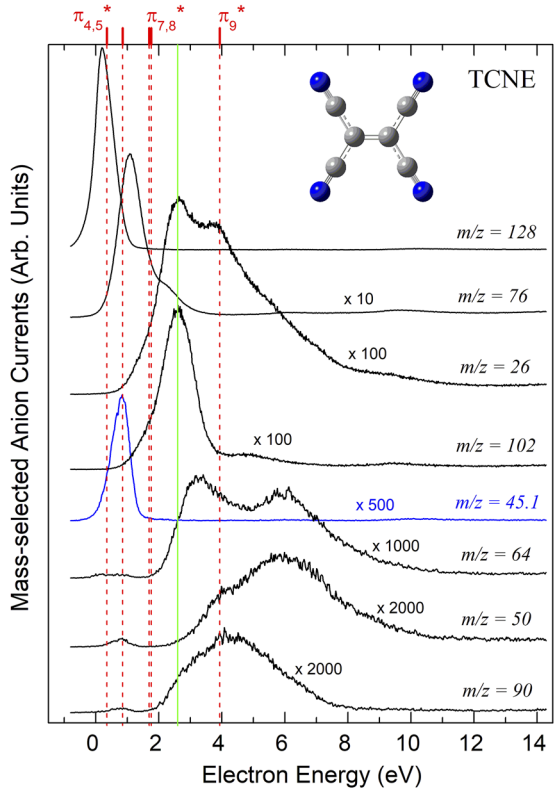

FIG. 1. Ion yield curves for TCNE in order of decreasing intensity. Vertical red dashed lines indicate predicted positions of shape resonances associated with e^- addition to the π^*_4–π^*_9 MOs, whereas the green solid line shows the position of the 2.6-eV ETS feature tentatively associated in the present study with core-excited resonance. The metastable anion current at m/z = 45.1 is marked in blue.

Electron attachment energies at which short-lived (femtoseconds) temporary negative ion states of TCNE, mostly associated with shape resonances,[1,2] can be formed have been reported by Burrow *et al.*[23] To the best of our knowledge, the DEA properties of TCNE have only been studied by means of experimental apparatus equipped with a monopole mass filter[24] that led to significant contributions to the measured negative ion signal from the hot filament surface ionization as well as from the electron current. In turn, the intense signal of molecular negative ions $TCNE^-$ has been observed up to 10 eV,[24] which *a priori* seems to be dubious under conditions of free electron attachment to this relatively small molecular target. The photochemistry and photon-stimulated fragmentation of gas-phase $TCNE^-$ have been studied by Khuseynov *et al.*[25] These authors also reported the adiabatic electron affinity (EA_a) of TCNE to be 3.16 ± 0.02 eV, the uncertainty being an order of magnitude below than that for previously reported EA_a values.[26,27] The EA_a evaluated using the electron-transfer equilibrium technique reported by Chowdhury and Kebarle is 3.17 eV,[26] whereas the value of 2.90 eV obtained by Chen and Wentworth[27] is likely somewhat underestimated. Christophorou *et al.* reported[28] electron detachment time (τ_a) from $TCNE^-$ to be in the μs-range using the time-of-flight technique.

The present paper is aimed at studying the formation of long-lived negative ions as well as the DEA properties of gas-phase TCNE by means of DEA spectroscopy.[1,2,29–31] The detection of metastable decay occurring on a microsecond timescale[32,33] shed some light on the dynamics of $TCNE^-$, which contains more than 3.5 eV of excess internal energy in its ground electronic but highly vibrationally excited state. Density functional theory methods are employed to calculate the thermodynamic energy thresholds for DEA-stimulated negative ion formation to describe the energetics of TCNE fragmentation by low-energy electrons as well as to predict the energy alignment of the vacant molecular orbitals (MOs).[34] The results are of interest to understand the behavior of this relatively small molecule widely used as a functional element in molecular magnets.[21,22] In these nanoscale devices, the TCNE molecule operates under conditions of excess negative charge; therefore, the DEA mechanism can lead to unpleasant surprises. For instance, as shown below, extra electron addition to TCNE is likely associated with the production of cyanogen, which is considered a highly toxic gas.[35] Since the DEA properties can be responsible for the long-term stability of nanoscale molecular assemblies,[36,37] the present findings are useful to overcome this primary obstacle on the way to the wide distribution of organic electronics devices.[38]

II. RESULTS AND DISCUSSION

A. General remarks

Currents of mass-selected negative ions formed in the gas-phase under single-collision conditions via a simple reaction TCNE + e^- → $TCNE^-$ → *Fragments*, where $TCNE^-$ stands for molecular anion, as a function of incident electron energy are shown in Fig. 1, the dependencies also being known as ion yield curves. Table I reports the likely structures of the observed negative fragments. The most intense signal is associated with the formation of long-lived molecular negative ions $TCNE^-$ (m/z = 128). It is to be noted that the flight time for the $TCNE^-$ species until their detection is estimated to be 27 μs under present experimental conditions. The elimination of CN^- negative species as well as two and one neutral CN radicals from $TCNE^-$ can be responsible for the generation of the most intense fragment anions detected at m/z = 26, 76, and 102, respectively, among the similar species detected in the photofragmentation study.[25] Other fragment anions observed at m/z = 50, 64, and 90 with lower intensity can be ascribed to the formation of $[TCNE - 3(CN)]^-$, rupture of the central C=C bond that divides the TCNE molecule in half, and elimination of CCN species from $TCNE^-$, respectively. The latter requires attachment of the CN group back to the molecular frame to produce the tricyanomethanide anion (m/z = 90). It is worth mentioning that migration of CN groups has been observed earlier in a DEA study of 2,3,5,6-tetrafluoro-7,7,8,8-tetracyanoquinodimethane.[39]

Table II reports B3LYP/6-31+G(d) total energies relative to the ground state of the neutral TCNE molecule (plus an electron in infinity) for anion and corresponding neutral fragment species likely formed by DEA to TCNE. In other words, Table II presents the estimated thermodynamic energy thresholds for the formation of these fragments. The suggested structures can explain the observed thresholds in the ion yield curves (Fig. 1), with the exception of very weak signals detected below 1 eV for the m/z = 50, 64, and 90 anions. However, the excess internal energy (vibrational plus

TABLE I. Probable structures of fragment negative ions observed in the DEA spectra of TCNE, peak energies (eV), and relative intensities (between parentheses) evaluated from the peak heights in order of decreasing mass numbers. The assignment of peak energies with the negative ion resonances is also reported (see Sec. II B); all values are in eV. Notes: sh. means shoulder; neutral stands for a peak observed in the signal of the neutral counterpart (see Sec. IV); VFR = Vibrational Feshbach Resonance; C.E. = Core-Excited Resonance; experimental VAEs are from the ETS study by Burrow *et al.* (see Ref. 23).

M/Z	Negative ion structure	Peak energy (relative intensity)					
128	$TCNE^-$	0.0 sh.	0.2 (100)	0.7 Neutral			
102	$[TCNE - CN]^-$				2.6 (0.8)		4.8 sh. 9.6 (<0.1)
90	$[TCNE - C(CN)]^-$			0.8 (<0.1)	3.0 sh.	4.3 (<0.1)	
76	$[TCNE - 2(CN)]^-$			1.1 (8.7)	2.3 sh.		6.0 (0.3) 9.7 (0.4)
64	$[TCNE - C(CN)_2]^-$		0.5 (<0.1)		3.3 (0.1)		6.0 (<0.1)
50	$[TCNE - 3(CN)]^-$			0.8 (<0.1)		4.0 sh.	6.0 (<0.1)
45.1	$m^*: 128 \rightarrow 76$			0.8 (0.1)			
26	CN^-				2.6 (1.1)	3.7 sh.	
	Negative ion resonance	VFR	$\pi_{4,5}^*$	π_6^*	C.E.	π_9^*	C.E.
	predicted VAE	<0	0.35	0.85		3.93	
	experimental VAE		0.5	0.96	2.6	4.6	

rotational) stored in the neutral TCNE molecule under the present experimental conditions, i.e., at 70 °C, is estimated to be 0.27 eV at the B3LYP/6-31+G(d) level of theory. The above-mentioned weak signals, therefore, can be explained (see, for instance, Ref. 40 and references therein) by electron attachment to vibrationally excited TCNE molecules.

B. Resonances in the DEA cross-section

The shapes of negative ion currents as a function of incident electron energy (Fig. 1) can be understood on the basis of vertical electron attachment energies (VAEs) measured in the total electron scattering cross-section of TCNE by means of electron transmission spectroscopy (ETS)[41,42] by Burrow *et al.*[23] In this study, most spectral features have been associated with electron addition to vacant MOs of TCNE via one-particle shape resonances;[1,2,30] therefore, the localization properties and energy alignment of these MOs are to be included in the discussion. B3LYP/6-31G(d) π^* virtual orbital energies (VOEs) of the TCNE molecule along with the VAEs predicted on the basis of empirical procedure[43] (see also Sec IV) are compared with ETS data in Table III. The present assignment of spectral features observed in the very complicated electron transmission spectrum of TCNE is somewhat different from that reported on the basis of the HF/3-21G calculations[23] since the established procedure to scale B3LYP/6-31G(d) VOEs is expected to provide much better predictions as reported in Table III. The mismatch between the energy of the broad and weak 4.6-eV ETS feature and the VAE (3.93 eV) predicted for the highest π_9^* shape resonance of the b_{2g} symmetry can be due to mixing with core-excited states (one-hole two-particle resonance).[1,2,30] Schematic representation and VAEs predicted for nine vacant π^* MOs of TCNE are illustrated in Fig. 2.

The predicted energies of the π_4^*–π_9^* MOs are also shown in Fig. 1 to match the observed peaks in the DEA cross-section. According to these data, the lowest π^* temporary negative ion that contains enough energy to allow dissociative decay of $TCNE^-$ is likely associated with electron addition to the π_6^* MO (predicted VAE = 0.85 eV). This state gives rise to the formation of metastable anions at the apparent m/z = 45.1 as well, but below its energy, the fragment anions are not observed with the exception of the m/z = 76, as shown in Table II and discussed below. Electron attachment to the lowest three π^* MOs (likely via vibrational Feshbach resonance) and to the $\pi_{4,5}^*$ MOs (via shape resonance) leads to the observation of only long-lived $TCNE^-$ species. Anion currents observed above 2 eV are likely due to the formation of the highest π_9^* negative ion state, which is expected to be mixed with core-excited resonances. The π_7^*

TABLE II. B3LYP/6-31+G(d) structures and total energies (eV) relative to the ground state of the neutral TCNE molecule. The values are corrected for zero-point vibrational energies.

	Fragment structures		
M/z	Negative ion	Neutral	Relative energy
128	$TCNE^-$ (vertical)		−3.39
128	$TCNE^-$ (adiabatic)		−3.51
102	$[TCNE - CN]^-$ 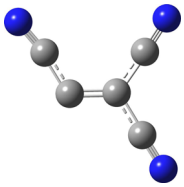	$^{\bullet}CN$	1.03
90	$[TCNE - C(CN)]^-$ (tricyanomethanide) 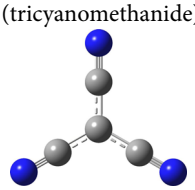	$^{\bullet}CCN$	1.24
76	$[TCNE - 2(CN)]^-$ 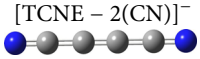	NCCN (cyanogen)	−0.35
		$^{\bullet}CN + {}^{\bullet}CN$	5.66
76	$[TCNE - 2(CN)]^-$ 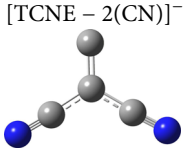	NCCN (cyanogen)	0.54
		$^{\bullet}CN + {}^{\bullet}CN$	6.55
64	$C(CN)_2^-$ 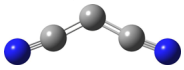	$^{\bullet}C(CN)_2$ 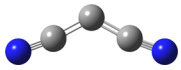	1.85
50	$[TCNE - 3(CN)]^-$ 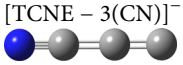	NCCN (cyanogen) + $^{\bullet}CN$	3.36
26	CN^-	$[TCNE - CN]^{\bullet}$ 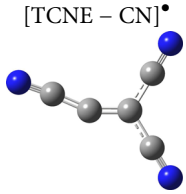	0.84

TABLE III. B3LYP/6-31G(d) virtual orbital energies (VOEs) for neutral TCNE; predicted and reported earlier experimental vertical attachment energies (VAEs) to form the negative ion π resonances. All values are in eV.

		VAE	
Orbital	VOE	Scaling[a]	ETS[b]
$\pi_9^*(b_{2g})$	3.737	3.93	4.6
$\pi_8^*(b_{3g})$	1.038	1.76	1.73
$\pi_7^*(b_{3u})$	0.955	1.69	1.53
$\pi_6^*(a_u)$	−0.082	0.85	0.96
$\pi_5^*(b_{1g})$	−0.705	0.35	0.5
$\pi_4^*(b_{2u})$	−0.706	0.35	
$\pi_3^*(b_{1u})$	−1.484	−0.28	
$\pi_2^*(a_g)$	−1.836	−0.56	
$\pi_1^*(b_{2g})$	−4.958	−3.08	

[a]VAE = 0.8065 × VOE + 0.9194 (see Ref. 43 and Sec IV).
[b]From ETS study by Burrow *et al.* (see Ref. 23).

and π_8^* resonances (predicted VAEs around 1.7 eV) are associated with shoulders in the DEA cross-section.

The most intense 2.6-eV ETS feature[23] cannot be associated with shape resonances on the basis of the present B3LYP/6-31G(d) calculations. Indeed, the predicted positions of both π_8^* (1.76 eV) and π_9^* (3.93 eV) MOs are far from 2.6 eV (see Fig. 2). The radical anion $TCNE^-$ shows a broad absorption feature centered around 2.9 eV,[44,45] with the corresponding vertical excitation energy for the transition from the ground 1^2B_{2g} $TCNE^-$ state to the 1^2B_{3u} state being calculated at 3.05 eV.[46] We, therefore, tentatively ascribe the 2.6-eV ETS feature to a core-excited resonance with two electrons in the lowest unoccupied MO and a hole in the highest occupied MO. The 2.6-eV resonance likely appears in the m/z = 26 and 102 anion currents as a peak as well as in the m/z = 64, 76, and 90 anion currents as a clearly seen shoulder (see the vertical solid green line in Fig. 1). The assignment of the negative ion resonances is also reported in Table I.

The predicted B3LYP/6-31+G(d) adiabatic electron affinity of TCNE (3.51 eV in Table II, obtained as the total energy difference between the neutral and the lowest anion state, each in its optimized geometry) is overestimated by 0.35 eV since the experimental value is reported to be 3.16 eV.[25] To correct the B3LYP/6-31+G(d) vertical electron affinity (3.39 eV in Table II, obtained as the difference between the total energy of the neutral and the lowest anion state, both in the optimized geometry of the neutral state), the calculated value is similarly decreased by 0.35 eV, which leads to 3.04 eV. This

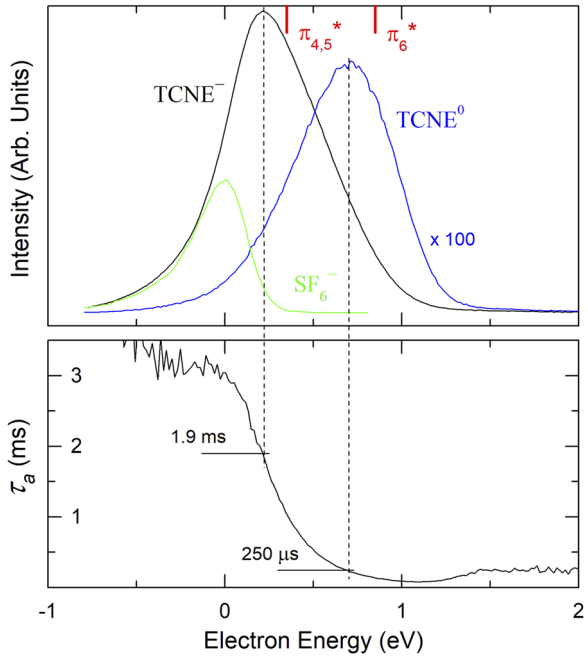

FIG. 3. Signals of molecular negative ions $TCNE^-$, corresponding neutral molecules $TCNE^0$ (blue line), and electron detachment time τ_a as a function of incident electron energy. The VAEs predicted for the π_4^*–π_6^* virtual orbitals are reported by red bars. The SF_6^- signal (green line) indicates the shape of the electron energy distribution.

value is in excellent agreement with the scaled π_1^* LUMO VAE (3.08 eV in Table III), which provides additional evidence that the scaling procedure[43] (see also Sec. IV) is correct. In turn, being confident in the scaling procedure, it can be concluded that not only the first 1^2A_g but also the second 1^2B_{1u} valence excited state of $TCNE^-$ is bound since the $\pi_2^*(a_g)$ and $\pi_3^*(b_{1u})$ temporary anion states (shape resonances) are predicted to lie in a bound region, their VAEs being predicted to be −0.56 and −0.28 eV, respectively, as reported in Table II. This conclusion contradicts that reported in the computational study,[46] however, and is in agreement with ETS results[23] as well as with predictions based on photodetachment data observed for CN-containing compounds.[47] In the present picture, the 0.5-eV ETS feature[23] should be associated with extra electron addition to practically degenerate π_4^* and π_5^* negative ion states, as presented in Table III.

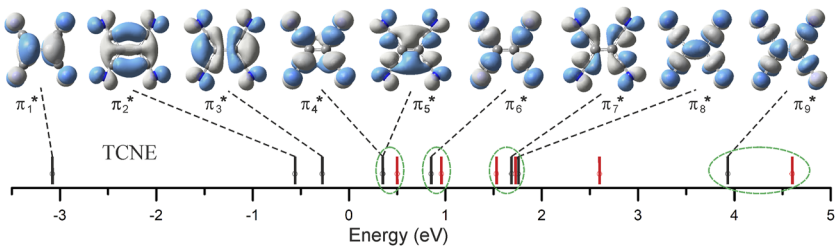

FIG. 2. B3LYP/6-31G(d) schematic representation and predicted VAEs (black bars) for virtual π^* MOs of neutral TCNE. Red bars indicate the positions of the spectral features detected by ETS.[23] Green ovals indicate the tentative assignment of the ETS features based on the predicted VAEs.

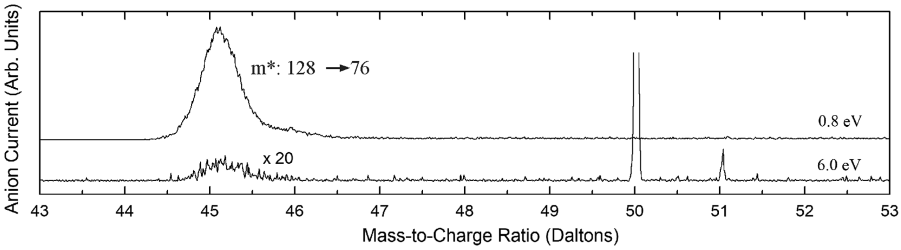

FIG. 4. Metastable broad anion peak observed at apparent (fractional) m/z = 45.1 in comparison with the normal narrow signal of the m/z = 50 anion species in the mass spectrum recorded at the fixed incident electron energies indicated in the figure.

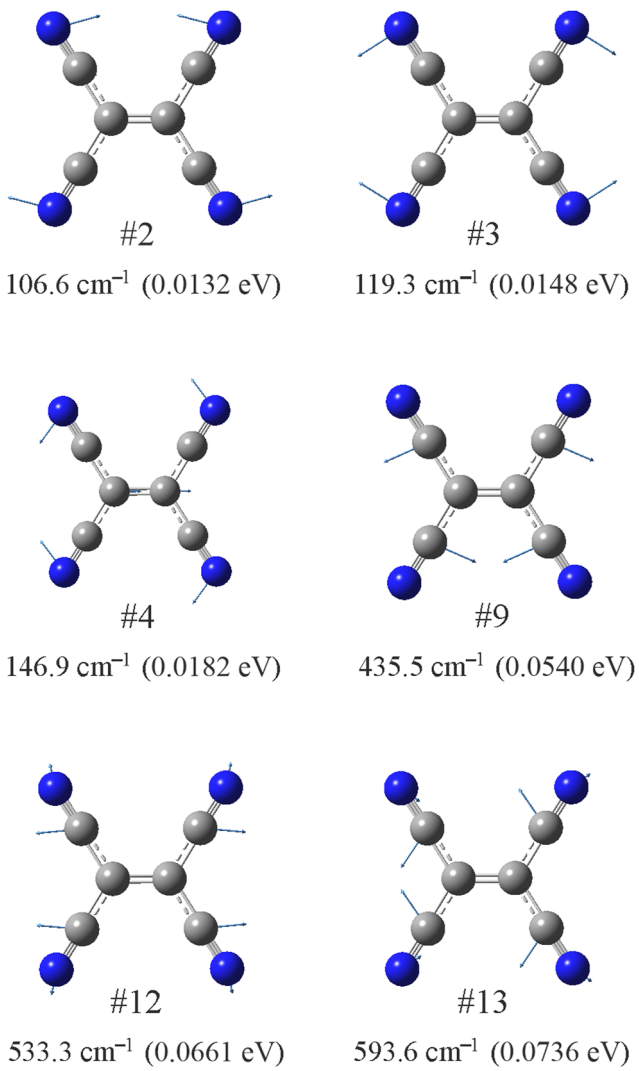

FIG. 5. B3LYP/6-31+G(d) schematic representation and vibrational quanta for low-frequency in plane fundamental vibrations of the TCNE molecule that allow carbon atoms of the CN groups to approach each other to form a cyanogen molecule that is a neutral counterpart for the m/z = 76 anion fragment. The displacement vectors are indicated by blue arrows.

C. Long-lived molecular anion and its slow decay

An interesting aspect of the present study concerns the observation of the long-lived $TCNE^-$ and its subsequent slow dissociation. This most intense decay is associated with the elimination of two CN groups to form the $[TCNE - 2(CN)]^-$ species (m/z = 76). A comparison between $TCNE^-$ current and that for the SF_6^- possessing an instrumental shape (see Fig. 3) leads to the conclusion that resonances with extra electron addition to almost degenerate π_4^* and π_5^* MOs (predicted VAE = 0.35 eV) give rise to the main peak in the $TCNE^-$ signal. Therefore, these excited temporary negative ion states can relax quickly (faster than electron autodetachment that usually appears on a femtosecond timescale) to the ground electronic state via internal conversions (radiationless transitions) as established for a variety of long-lived molecular anions.[48–50] In fact, the final 1^2B_{2g} $TCNE^-$ state is able to keep excess electron on a milli- to microsecond timescale, as reported in Fig. 3.

Electron attachment to the π_1^*–π_3^* MOs predicted to lie in the bound region likely via vibrational Feshbach resonance[2,3,29,31] is expected to be responsible for the left wing of the broad 0.2-eV peak in $TCNE^-$ current. This contribution, however, is unresolved in the present data due to low electron energy resolution. On the contrary, the contribution of the π_6^* shape resonance (predicted VAE = 0.85 eV) to the right wing of the $TCNE^-$ current prolonged above 1 eV is clearly supported by the observation of a 0.7-eV peak in the $TCNE^0$ signal as shown in Fig. 3. This signal is due to neutral particles (labeled $TCNE^0$) formed by electron detachment from the relaxed $TCNE^-$ initially formed in the π_6^* anion state. Indeed, $TCNE^- \rightarrow TCNE^0 + e^-$ process occurs not only in the collision cell but, in particular, when mass-selected $TCNE^-$ anions fly through the fields-free area located between the mass analyzing magnet and the detection system (see Sec IV). According to the present data, electron detachment from $TCNE^-$ observed at 0.7 and 0.5 eV occurs in 250 and 550 μs, respectively, whereas the $TCNE^-$ formed close to thermal energy (0.2 eV) is able to keep excess electron on a millisecond timescale (~1.9 ms, see Fig. 3).

The lowest negative ion state that gives rise to the fragmentation of TCNE via the DEA mechanism is associated with electron addition into the π_6^* MO. In fact, only long-lived $TCNE^-$ species are observed below the predicted energy (0.85 eV in Table III) of the π_6^* resonance as presented in Fig. 1. Electron addition to the π_6^* MO leads to the formation of only negative fragments $[TCNE - 2(CN)]^-$ observed either as a normal mass peak at m/z = 76 or as metastable anions in a broad mass peak at apparent m/z = 45.1

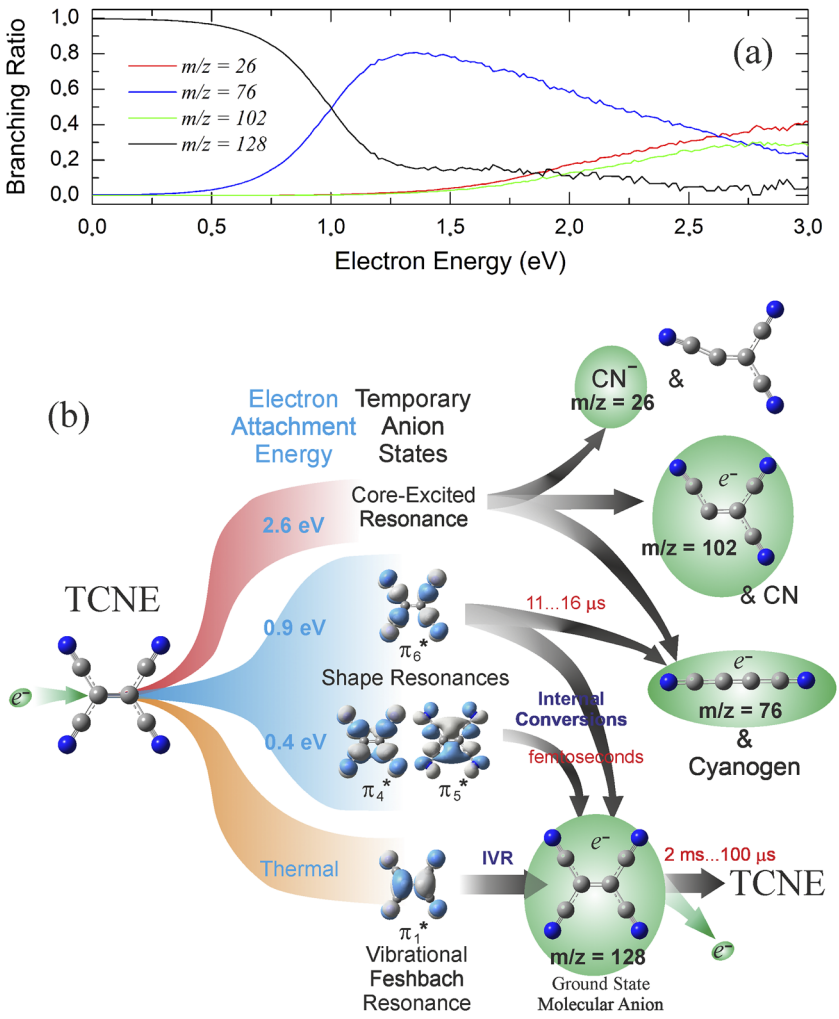

FIG. 6. The branching ratio curves (a) and schematic representation (b) for the generation of the most abundant negative ions produced by resonance electron attachment to gas-phase TCNE. The temporary negative ion states involved in these decays as well as characteristic timescales are also indicated. IVR stands for internal vibrational energy redistribution.

(Fig. 4). It is to be noted that the simple rupture of a single bond with the formation of either CN^- (m/z = 26) or $[TCNE - CN]^-$ (m/z = 102) is a priori expected to be kinetically more efficient. However, experimental findings indicate that the elimination of two CN groups from $TCNE^-$ to form the m/z = 76 species produces a signal an order of magnitude higher than that for the m/z = 26 or m/z = 102 (see Fig. 1).

According to the B3LYP/6-31+G(d) thresholds, the elimination of two separate CN groups is expected to occur at incident electron energy above 5.66 eV (Table II), whereas the m/z = 76 and 45.1 currents peak at 1.1 and 0.8 eV, respectively. Therefore, it should be concluded that the formation of $[TCNE - 2(CN)]^-$ is accompanied by the elimination of its neutral counterpart in the form of the closed-shell NCCN (cyanogen) molecule. The present B3LYP/6-31+G(d) calculations predict a negative threshold in this case, provided that the m/z = 76 anion is in its linear form; in other words, CN groups are eliminated from the neighbor carbon atoms as presented in Table II. This process leads to an energy release of 0.35 eV and is expected to be energetically and kinetically more favorable. Indeed, the whole process requires CN groups to approach each other to be eliminated as a cyanogen molecule.

There are several fundamental vibrations of the TCNE molecule that allow the cyano groups to approach each other (Fig. 5), which, therefore, can favor their elimination as a cyanogen molecule. Since the vibrational quanta are calculated to be small (see Fig. 5), these vibrations are expected to be strongly populated in $TCNE^-$, the calculated frequencies of which are very close to those of TCNE. Evidently, cyanogen formation is expected to occur more easily if the CN groups are eliminated from the neighbor carbon atoms. Therefore, despite the fact that the formation of a triangular m/z = 76 structure is also possible on energetic grounds (predicted threshold = 0.54 eV), this structure seems to be less probable kinetically.

To illustrate the $TCNE^-$ decays, Fig. 6(a) reports the branching ratio curves for the generation of the most abundant negative

ions via competitive processes dominant at incident electron energies below 1.5 eV, namely, the formation of the long-lived anion $TCNE^-$ (m/z = 128) and its dissociation with the generation of the $[TCNE - 2(CN)]^-$ fragment (m/z = 76). Two complementary decays of $TCNE^-$ associated with the elimination of a cyano group in its negatively charged form (m/z = 26) or as a neutral counterpart of the m/z = 102 negative ion dominate the DEA signals as incident electron energy exceeds 2.7 eV. It is interesting to note that approximately half of the $TCNE^-$ anions formed close to 1 eV, i.e., by electron addition into the π_6^* MO, dissociate by elimination of a cyanogen molecule, whereas the latter half decays by autodetachment of an extra electron in ~100 μs (see Fig. 3).

Finally, the extraction time of $TCNE^-$ from the collision cell is estimated at 11 μs, and their flight time through the field-free area located between the acceleration region and mass analyzer is 16 μs under the present experimental conditions.[29,33] Therefore, it should be concluded that $TCNE^-$ observed around 0.8 eV, i.e., in the maximum of the m/z = 45.1 current, can dissociate in 11–16 μs with the formation of $[TCNE - 2(CN)]^-$ species more likely in their linear form. Increasing incident electron energy above 0.8 eV makes this process faster, which leads to the observation of the m/z = 76 normal signal in the 1.1-eV peak. This signal is associated with the dissociation of $TCNE^-$ inside the collision cell, i.e., faster than 11 μs from its formation. Decreasing incident electron energy below 0.8 eV suppresses the dissociative decays that lead to the observation of the long-lived anion $TCNE^-$, which detaches extra electrons in 250 μs as measured at 0.7 eV (Fig. 3). We tentatively attribute these three processes (slow dissociation, fast dissociation, and electron detachment) to the formation of the π_6^* temporary anion state on the basis of its predicted (0.85 eV) and experimental (0.96 eV) VAEs as well as the observed peaks in the anion currents. These competing processes provide a delicate balance between slow and fast decays of the $TCNE^-$ formed by resonance electron attachment to the π_6^* virtual orbital via either dissociation or electron autodetachment. To summarize these findings, the abundant $TCNE^-$ competitive decays, including electron autodetachment and dissociation, are illustrated in Fig. 6(b).

III. CONCLUSIONS

Free low-energy (0–15 eV) electron interaction with gas-phase TCNE via resonance mechanisms is studied by means of DEA spectroscopy. Experimental findings are assigned based on density functional theory calculations. The predicted electron attachment energies to form temporary anion states of TCNE are compared with previously reported ETS data. On this basis, the main conclusions are the following:

(1) Despite the TCNE molecule being relatively small, the long-lived, i.e., mass spectrometrically observable on a microsecond timescale, molecular negative ions $TCNE^-$ are detected in a broad range of the incident electron energies, in particular at epithermal energies corresponding to the formation of shape resonances with extra electron addition into the π_4^*–π_6^* MOs (predicted VAEs of 0.35–0.85 eV).
(2) A variety of dissociative decays of $TCNE^-$, mostly associated with the elimination of the cyano groups, are detected at incident electron energies above 1.7 eV, i.e., in the energy range of the π_7^*–π_9^* temporary negative ion states with likely contributions from core-excited resonances.
(3) The 2.6-eV ETS feature lying in the gap between the predicted positions for the π_8^* (1.76 eV) and π_9^* (3.93 eV) shape resonances can be associated with the core-excited $TNCE^-$ state.
(4) Not only the first 1^2A_g but also the second 1^2B_{1u} valence excited state of $TCNE^-$ is bound.
(5) The most intense and energetically beneficial DEA channel is associated with the elimination of two cyano groups from the $TCNE^-$ (m/z = 128) to form the $[TCNE - 2(CN)]^-$ species (m/z = 76). This rearrangement process competing with electron autodetachment appears on a microsecond timescale; the conclusion is supported by the observation of metastable anions in broad mass peaks at the m/z = 45.1.
(6) Extra electron addition into the π_6^* vacant MO contributes to the DEA cross-section in a relatively narrow electron energy range (0.7–1.1 eV) and produces cyanogen since, on energetic grounds, only the NCCN closed-shell structure can be formed as a neutral counterpart for the m/z = 76 anion.
(7) DEA can not only prevent the long-term stability of TCNE-based nanoscale magnets but also provide a source of harmful effects via the generation of toxic gaseous species, provided that an organic electronics device operates under conditions of excess negative charge.

IV. EXPERIMENTAL AND COMPUTATIONAL METHODS

An overview of DEA spectroscopy (DEAS) may be found elsewhere,[1,2,30,31] and specific conditions of the present technique are described in Refs. 29 and 33. Briefly, a low-energy (0–15 eV) electron beam is passed through a collision cell filled with a vapor of the compound under investigation, as schematically presented in Fig. 7. A current (I) of mass-selected (using a sector magnetic analyzer) negative ions is registered as a function of the incident electron energy (ε). The electron energy scale is calibrated by detecting the SF_6^- current formed by thermal electron attachment to SF_6. The full width at half maximum of the electron energy distribution is estimated to be 0.4 eV, and the accuracy of the measured peaks is estimated to be ±0.1 eV. The substance under investigation (TCNE, Sigma-Aldrich No. T8809, 96%) was evaporated at 45 °C, which is far below its melting point (199 °C). The minimal possible temperature of the collision cell was 70 °C due to heating from the hot filament.

Metastable anions are registered as broad signals in the mass spectrum and indicate a slow decay between the initial (m_1^-) and final (m_2^-) negative fragments, i.e., the process $m_1^- \rightarrow m_2^- + Neutral$, which takes place in the acceleration region (microsecond timescale). The apparent m/z ratio (m^*) of a metastable peak can be estimated by means of the equation $m^* = m_2^2/m_1$.[32] The evaluation of the electron detachment time (τ_a) is based on the detection of the neutral species formed by electron detachment from negative ions during their flight through the field-free region between

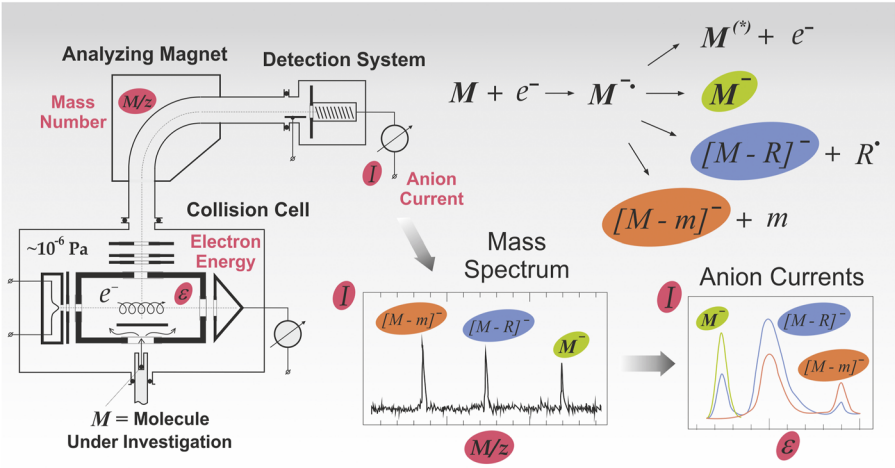

FIG. 7. Schematic representation of the DEA spectroscopy and DEA process. The main parameters of the experiment, incident electron energy (ε) and mass number (M/z), as well as the measured signal, mass-selected anion currents (I), are indicated.

the mass-analyzer and the detection system (see Fig. 7), as proposed for time-of-flight experiments[51] and modified for magnetic mass spectrometers.[29] The accuracy of the measured electron detachment times is ±20% provided that the measured signals lie in the experimental time window (tens of hundred microseconds) that allows detection of the neutral counterpart. The evaluated detachment times should be referred to as those determined for a test compound, for instance, sulfur hexafluoride.[49,50] Under the present experimental conditions (70 °C), the electron detachment time for the SF_6^- was 120 μs.

The density functional theory calculations were performed with the Gaussian 09.[52] Regardless of the difficulties encountered in the calculations of negative ion states,[53] it has been reported[54–56] that linear correlations can be obtained between experimental VAEs and the corresponding VOEs of neutral molecules calculated with basis sets without diffuse functions. In particular, the scaling of σ^* and π^* MOs requires different parameters, and the correlation is more accurate provided that "training" compounds are structurally similar to the subject molecule.[34,57] In the present study, the linear equation VAE = 0.8065 × VOE + 0.9194[43] was employed to obtain the B3LYP/6-31G(d) π^* VAEs.

The first vertical electron affinity of TCNE was estimated as the difference between the total energy of the neutral and the lowest anion state, both in the optimized geometry of the neutral TCNE, using the B3LYP functional[58] with a 6-31+G(d) basis set with the minimum addition of diffuse functions. The adiabatic electron affinity of TCNE was estimated as the energy difference between the neutral and the lowest anion state, each in its optimized geometry. To assign the structures of the fragments observed in DEA spectra, the thermodynamic energy thresholds were calculated as the difference between the total energies of the negatively charged and neutral fragment species and that of the neutral ground state at the B3LYP/6-31+G(d) level of theory.

ACKNOWLEDGMENTS

This study was performed with the support of the Russian Science Foundation (Project No. 19-13-00021). The authors are grateful to the reviewers for their useful comments and suggestions.

AUTHOR DECLARATIONS

Conflict of Interest

The authors have no conflicts to disclose.

Author Contributions

Stanislav A. Pshenichnyuk: Investigation (equal); Writing – original draft (equal); Writing – review & editing (equal). **Nail L. Asfandiarov**: Investigation (equal); Writing – original draft (equal); Writing – review & editing (equal). **Rustam G. Rakhmeyev**: Investigation (equal); Writing – original draft (equal); Writing – review & editing (equal). **Aleksey M. Safronov**: Investigation (equal). **Alexei S. Komolov**: Investigation (equal); Writing – original draft (equal); Writing – review & editing (equal).

DATA AVAILABILITY

The data that support the findings of this study are available from the corresponding author upon reasonable request.

REFERENCES

[1] G. J. Schulz, "Resonances in electron impact on diatomic molecules," Rev. Mod. Phys. **45**(3), 423 (1973).
[2] L. G. Christophorou, *Electron–Molecule Interactions and their Applications* (Academic Press, Orlando, 1984), Vol. 2.
[3] I. I. Fabrikant, S. Eden, N. J. Mason, and J. Fedor, "Recent progress in dissociative electron attachment: From diatomics to biomolecules," Adv. At., Mol., Opt. Phys. **66**, 545–657 (2017).
[4] E. Alizadeh and L. Sanche, "Precursors of solvated electrons in radiobiological physics and chemistry," Chem. Rev. **112**(11), 5578–5602 (2012).
[5] I. Baccarelli, I. Bald, F. A. Gianturco, E. Illenberger, and J. Kopyra, "Electron-induced damage of DNA and its components: Experiments and theoretical models," Phys. Rep. **508**(1-2), 1–44 (2011).
[6] S. A. Pshenichnyuk, A. Modelli, and A. S. Komolov, "Interconnections between dissociative electron attachment and electron-driven biological processes," Int. Rev. Phys. Chem. **37**(1), 125–170 (2018).

[7]Y. Zhang, S. He, W. Guo, Y. Hu, J. Huang, J. R. Mulcahy, and W. D. Wei, "Surface-plasmon-driven hot electron photochemistry," Chem. Rev. **118**(6), 2927–2954 (2017).
[8]C. R. Arumainayagam, H.-L. Lee, R. B. Nelson, D. R. Haines, and R. P. Gunawardane, "Low-energy electron-induced reactions in condensed matter," Surf. Sci. Rep. **65**(1), 1–44 (2010).
[9]D. Shen, W.-C. Chen, M.-F. Lo, and C.-S. Lee, "Charge-transfer complexes and their applications in optoelectronic devices," Mater. Today Energy **20**, 100644 (2021).
[10]P. Kebarle and S. Chowdhury, "Electron affinities and electron-transfer reactions," Chem. Rev. **87**(3), 513–534 (1987).
[11]E. C. M. Chen and W. E. Wentworth, "A comparison of experimental determinations of electron affinities of pi charge transfer complex acceptors," J. Chem. Phys. **63**(8), 3183–3191 (1975).
[12]R. Balog, J. Langer, S. Gohlke, M. Stano, H. Abdoul-Carime, and E. Illenberger, "Low energy electron driven reactions in free and bound molecules: From unimolecular processes in the gas phase to complex reactions in a condensed environment," Int. J. Mass Spectrom. **233**(1-3), 267–291 (2004).
[13]*Low-Energy Electrons: Fundamentals and Applications*, edited by O. Ingólfsson (CRC Press, 2019).
[14]M. Y. Wong and E. Zysman-Colman, "Purely organic thermally activated delayed fluorescence materials for organic light-emitting diodes," Adv. Mater. **29**(22), 1605444 (2017).
[15]N. Martín, J. L. Segura, and C. Seoane, "Design and synthesis of TCNQ and DCNQI type electron acceptor molecules as precursors for 'organic metals,'" J. Mater. Chem. **7**(9), 1661–1676 (1997).
[16]M. S. Liu, X. Jiang, P. Herguth, and A. K.-Y. Jen, "Efficient cyano-containing electron-transporting polymers for light-emitting diodes," Chem. Mater. **13**(11), 3820–3822 (2001).
[17]J. O. Egekeze and F. W. Oehme, "Cyanides and their toxicity: A literature review," Vet. Q. **2**(2), 104–114 (1980).
[18]S. N. Vogel, T. R. Sultan, and R. P. Ten Eyck, "Cyanide poisoning," Clin. Toxicol. **18**(3), 367–383 (1981).
[19]Z. Song and X. Xu, "Advanced research on anti-tumor effects of amygdalin," J. Cancer Res. Ther. **10**(5), 3 (2014).
[20]D. A. Jones, "Why are so many food plants cyanogenic?," Phytochemistry **47**(2), 155–162 (1998).
[21]R. Jain, K. Kabir, J. B. Gilroy, K. A. R. Mitchell, K.-c. Wong, and R. G. Hicks, "High-temperature metal–organic magnets," Nature **445**(7125), 291–294 (2007).
[22]Y. Huang, Y. Hu, L. An, Z. Li, J. N. Armstrong, and S. Ren, "Electron transfer induced magnetic ordering of metal-cyanide magnets," Mater. Adv. **1**(5), 1061–1065 (2020).
[23]P. D. Burrow, A. E. Howard, A. R. Johnston, and K. D. Jordan, "Temporary anion states of hydrogen cyanide, methyl cyanide, and methylene dicyanide, selected cyanoethylenes, benzonitrile, and tetracyanoquinodimethane," J. Phys. Chem. **96**(19), 7570–7578 (1992).
[24]C. E. Brion and L. A. R. Oslen, "Negative-ion formation in tetracyanoethylene," Int. J. Mass Spectrom. Ion Phys. **9**(4), 413–416 (1972).
[25]D. Khuseynov, M. T. Fontana, and A. Sanov, "Photoelectron spectroscopy and photochemistry of tetracyanoethylene radical anion in the gas phase," Chem. Phys. Lett. **550**, 15–18 (2012).
[26]S. Chowdhury and P. Kebarle, "Electron affinities of di- and tetracyanoethylene and cyanobenzenes based on measurements of gas-phase electron-transfer equilibria," J. Am. Chem. Soc. **108**(18), 5453–5459 (1986).
[27]E. C. M. Chen and W. E. Wentworth, "Experimental determination of electron affinities of organic molecules," Mol. Cryst. Liq. Cryst. **171**(1), 271–285 (1989).
[28]L. G. Christophorou, A. Hadjiantonious, and J. G. Carter, "Long-lived parent negative ions formed via nuclear-excited Feshbach resonances. Part 3. Variation of the autodetachment lifetime with incident electron energy," J. Chem. Soc., Faraday Trans. 2 **69**, 1713–1722 (1973).
[29]V. I. Khvostenko, *Negative Ions Mass Spectrometry in Organic Chemistry* (Nauka, Moscow, 1981) (in Russian).
[30]M. Allan, "Study of triplet states and short-lived negative ions by means of electron impact spectroscopy," J. Electron Spectrosc. Relat. Phenom. **48**(2), 219–351 (1989).
[31]E. Illenberger and J. Momigny, *Gaseous Molecular Ions: An Introduction to Elementary Processes Induced by Ionization* (Steinkopff Verlag Darmstadt, Springer-Verlag, New York, 1992).
[32]J. H. Beynon, *Mass Spectrometry and its Application to Organic Chemistry* (Elsevier, Amsterdam, 1960).
[33]S. A. Pshenichnyuk, N. L. Asfandiarov, A. S. Vorob'ev, and Š. Matejčík, "State of the art in dissociative electron attachment spectroscopy and its prospects," Phys.-Usp. **65**(2), 163–188 (2022).
[34]P. D. Burrow and A. Modelli, "On the treatment of LUMO energies for their use as descriptors," SAR QSAR Environ. Res. **24**(8), 647–659 (2013).
[35]J. M. McNerney and H. H. Schrenk, "The acute toxicity of cyanogen," Am. Ind. Hyg. Assoc. J. **21**(2), 121–124 (1960).
[36]A. Modelli and P. D. Burrow, "Electron attachment to dye-sensitized solar cell components: Cyanoacetic acid," J. Phys. Chem. A **115**(6), 1100–1107 (2011).
[37]A. Modelli, D. Jones, and S. A. Pshenichnyuk, "Electron attachment to dye-sensitized solar cell components: Rhodanine and rhodanine-3-acetic acid," J. Phys. Chem. C **114**(3), 1725–1732 (2010).
[38]E. K. Lee, M. Y. Lee, C. H. Park, H. R. Lee, and J. H. Oh, "Toward environmentally robust organic electronics: Approaches and applications," Adv. Mater. **29**(44), 1703638 (2017).
[39]S. A. Pshenichnyuk, A. Modelli, N. L. Asfandiarov, R. G. Rakhmeyev, A. M. Safronov, M. M. Tayupov, and A. S. Komolov, "Microsecond dynamics of molecular negative ions formed by low-energy electron attachment to fluorinated tetracyanoquinodimethane," J. Chem. Phys. **155**, 184301 (2021).
[40]W. Sailer, A. Pelc, M. Probst, J. Limtrakul, P. Scheier, E. Illenberger, and T. D. Märk, "Dissociative electron attachment to acetic acid (CH_3COOH)," Chem. Phys. Lett. **378**(3-4), 250–256 (2003).
[41]L. Sanche and G. J. Schulz, "Electron transmission spectroscopy: Rare gases," Phys. Rev. A **5**(4), 1672 (1972).
[42]K. D. Jordan and P. D. Burrow, "Temporary anion states of polyatomic hydrocarbons," Chem. Rev. **87**(3), 557–588 (1987).
[43]A. M. Scheer and P. D. Burrow, "π^* orbital system of alternating phenyl and ethynyl groups: Measurements and calculations," J. Phys. Chem. B **110**(36), 17751–17756 (2006).
[44]N. Okumura, M. Goto, and B. Uno, "Structural and spectral characteristics of the electrogenerated tetracyanoethylene dianion," Chem. Pharm. Bull. **48**(4), 537–541 (2000).
[45]D. A. Dixon and J. S. Miller, "Crystal and molecular structure of the charge-transfer salt of decamethylcobaltocene and tetracyanoethylene (2:1):{[Co$(C_5Me_5)_2]^+$}$_2[(NC)_2CC(CN)_2]^{2-}$. The electronic structures and spectra of $[TCNE]^n$ (n = 0, 1−, 2−)," J. Am. Chem. Soc. **109**(12), 3656–3664 (1987).
[46]B. Milián, R. Pou-Amérigo, M. Merchán, and E. Ortí, "Theoretical study of the electronic excited states of tetracyanoethylene and its radical anion," ChemPhysChem **6**(3), 503–510 (2005).
[47]E. A. Brinkman, E. Günther, O. Schafer, and J. I. Brauman, "Bound excited electronic states of anions," J. Chem. Phys. **100**(3), 1840–1848 (1994).
[48]S. A. Pshenichnyuk, A. S. Vorob'ev, and A. Modelli, "Resonance electron attachment and long-lived negative ions of phthalimide and pyromellitic diimide," J. Chem. Phys. **135**(18), 184301 (2011).
[49]A. S. Vorob'ev, S. A. Pshenichnyuk, N. L. Asfandiarov, and E. P. Nafikova, "Internal conversion as the main stabilization mechanism for long-lived negative molecular ions," Tech. Phys. **59**(9), 1277–1285 (2014).
[50]S. A. Pshenichnyuk, A. S. Vorob'ev, N. L. Asfandiarov, and A. Modelli, "Molecular anion formation in 9, 10-anthraquinone: Dependence of the electron detachment rate on temperature and incident electron energy," J. Chem. Phys. **132**(24), 244313 (2010).
[51]D. Edelson, J. E. Griffiths, and K. B. McAfee, Jr., "Autodetachment of electrons in sulfur hexafluoride," J. Chem. Phys. **37**(4), 917–918 (1962).
[52]M. J. Frisch *et al.*, Gaussian 09, Revision A.02, Gaussian, Inc., Wallingford CT, 2009.
[53]J. Simons and K. D. Jordan, "Ab initio electronic structure of anions," Chem. Rev. **87**(3), 535–555 (1987).
[54]S. W. Staley and J. T. Strnad, "Calculation of the energies of π^* negative ion resonance states by the use of Koopmans' theorem," J. Phys. Chem. **98**(1), 116–121 (1994).

[55]D. Chen and G. A. Gallup, "The relationship of the virtual orbitals of self-consistent-field theory to temporary negative ions in electron scattering from molecules," J. Chem. Phys. **93**(12), 8893–8901 (1990).
[56]A. Modelli, "Electron attachment and intramolecular electron transfer in unsaturated chloroderivatives," Phys. Chem. Chem. Phys. **5**(14), 2923–2930 (2003).
[57]S. A. Pshenichnyuk, N. L. Asfandiarov, and P. D. Burrow, "A relation between energies of the short-lived negative ion states and energies of unfilled molecular orbitals for a series of bromoalkanes," Russ. Chem. Bull. **56**, 1268–1270 (2007).
[58]A. D. Beeke, "Density-functional thermochemistry. III. The role of exact exchange," J. Chem. Phys. **98**(7), 5648–5652 (1993).